Journal of The Electrochemical Society, **146** (12) 4455-4460 (1999)
S0013-4651(99)01-006-X CCC: $7.00 © The Electrochemical Society, Inc.

Atomic Force Microscopy Study of Microbiologically Influenced Corrosion of Mild Steel

Li-Chong Xu,[a] Herbert H. P. Fang,[a] and Kwong-Yu Chan[b,*,z]

[a]*Department of Civil Engineering and* [b]*Department of Chemistry, The University of Hong Kong, Hong Kong*

The anaerobic corrosion of mild steel in seawater was studied by atomic force microscopy (AFM). In the presence of sulfate reducing bacteria (SRB), corrosion was intensified and accelerated. A biofilm consists of heterogeneous microbial cells and extracellular polymeric substance with interstitial voids was observed on the surface of mild steel coupons. The greatest damage of steel occurred beneath the biofilm, in the form of pitting corrosion. The corrosion of steel can be quantified through section and bearing analyses. The depth of pits increased linearly with time whereas the volume of pits increased as $t^{2.83}$, the 2.83 power of time. Compared with a control experiment without SRB, the depth of pitting corrosion is about one order of magnitude higher. Weight loss estimates from AFM images are about one order of magnitude smaller than actual weight loss experimental results. The problems of AFM quantification of corrosion rate at extended stage of corrosion are discussed.

Manuscript submitted January 8, 1999; revised manuscript received July 29, 1999.

Microbiologically influenced corrosion (MIC) of metals is common in the natural aquatic environment. It is estimated that about 20% of corrosion is due to MIC.[1] The activity of microorganisms changes the local conditions near the surface of a metal substrate, and corrosion is accelerated. Microorganisms attach themselves to the surface of materials, colonize, proliferate, and produce a biofilm. Gradients of pH, dissolved oxygen, chloride, and sulfate[2,3] exist in the biofilm, and localized corrosion conditions are created. The development of biofilm usually results in pitting, crevice corrosion, selective dealloying, stress corrosion cracking, or under-deposit corrosion.[4] The metabolic products of certain microorganism may also be corrosive to the metal substrate, and the secreted enzymes may serve as catalysts of corrosion. For example, the high specific activity of the enzyme hydrogenase was found in a biofilm formed on mild steel by an aggressive sulfate reducing bacteria isolate.[5] Iron oxidizing,[6] manganese oxidizing,[7,8] sulfur oxidizing,[9] iron reducing,[10] sulfate reducing bacteria,[4,5] and other physiological groups, have been recognized for corrosion of metals and alloys. The most widely recognized and studied bacteria in MIC, however, are the sulfate-reducing bacteria (SRB) which consist of a diverse and ecologically interactive group of anaerobic prokaryotes. They share an extraordinary trait: growth by sulfate respiration with hydrogen sulfide as the major end product. Sulfide has been known to cause cathodic hydrogen depolarization and may also damage the passivity of stainless steel by accelerating anodic interaction.[11,12] The extracellular polymeric substance (EPS) secreted by SRB facilitates irreversible cell attachment leading to colonization on the steel surface. It also binds metal ions, resulting in metal ion concentration cells and changing the electrochemical condition of the steel surface.[13,14]

MIC has the common forms of corrosion. Investigators have relied on the shape, morphology, color, and smell of surface deposits to characterize MIC. It is still unclear what the key mechanisms involved in MIC are. Electrochemical methods for studying MIC include direct current methods, alternating current impedance spectroscopy, and electrochemical noise measurements. These methods assume the chemical and electrochemical conditions on the metal surface are uniform.[15-17] In reality, biofilms tend to create nonuniform surface conditions leading to localized corrosion, usually in the form of pitting. Atomic force microscopy (AFM) has been useful in elucidating corrosion phenomena related to biofilms on metals surface. Using AFM, Bremmer *et al.*[18] observed bacteria colonization on both polished and unpolished copper surfaces under batch culture conditions. Bacterial cells were shown to be associated with pits on the surface of unpolished copper. Corrosion of 316L stainless steel under the biofilm of a consortium of SRB, aerobes, and bacteria isolated from a corroded pipework was studied by Steele *et al.*[19] and the direct visualizations of submicrometer features of marine SRB cells on mica were carried out. Beech *et al.*[20] also reported AFM study of SRB biofilms which induced corrosion on steel surface. While AFM images and analyses have been reported, no determination of corrosion rate has been made using AFM analyses.

This paper reports an AFM study of marine SRB biofilm on mild steel and the induced corrosion under laboratory conditions. The changes in depth and volume of pits are examined and results are compared with weight loss.

Experimental

Preparation of coupons.—Mild steel coupons (10 × 10 × 1.5 mm) were used for AFM study and coupons of 40 × 15 × 1.5 mm were used for weight loss measurements. The coupons were wet polished with a series of grit SiC paper (320, 400, 600, 800), followed by degreasing with ethanol, drying in ambient air, and storage in a desiccator prior to use. The coupons used for AFM study were further polished with 0.3 μm alumina particles.

Preparation of seawater and SRB culture.—Seawater was taken from the Victoria Harbour, Hong Kong, and sterilized by filtering through the 0.45 μm membrane before use. The seawater contains 2200 mg sulfate ions per liter as analyzed by ion chromatography. The SRB seed was isolated from marine sediment and cultured in modified Postgate's medium C [21] at room temperature. Each liter of seawater contained 0.5 g KH_2PO_4, 1 g NH_4Cl, 0.06 g $CaCl_2 \cdot 6H_2O$; 0.06 g $MgSO_4 \cdot 7H_2O$, 6 mL sodium lactate (70%); 1 g yeast extract; 0.004 g $FeSO_4 \cdot 7H_2O$; and 0.3 g sodium citrate. The pH was adjusted to 7.2 ± 0.1 using 1 M NaOH solution.

Development of biofilms and corrosion in SRB cultures.—Each liter of test solution contains the SRB culture with addition of 1 mL of resazurin solution (0.1%) and the control solution is sterilized seawater with resazurin solution but no SRB. All experiments were carried out in enclosed 1 L glass reactors. The solutions were autoclaved at 121°C for 15 min. After autoclaving, the solution was flushed with pure N_2 to remove dissolved oxygen. Resazurin changes color from violet to orange and then becomes colorless indicating removal of oxygen from the system. For each liter of test solution, 10 mL SRB seed were added. The test coupons hung on the Nylon strings were then immersed. Half of the test solution was replaced with fresh oxygen-free sterile solution once a week. On days 10, 20, 30, 40, 50, and 60, separate coupons were taken out for AFM examination and weight loss measurements were carried out on days 15, 30, 45, 60, and 75.

* Electrochemical Society Active Member.
z E-mail: hrsccky@hku.hk

S0013-4651(99)01-006-X CCC: $7.00

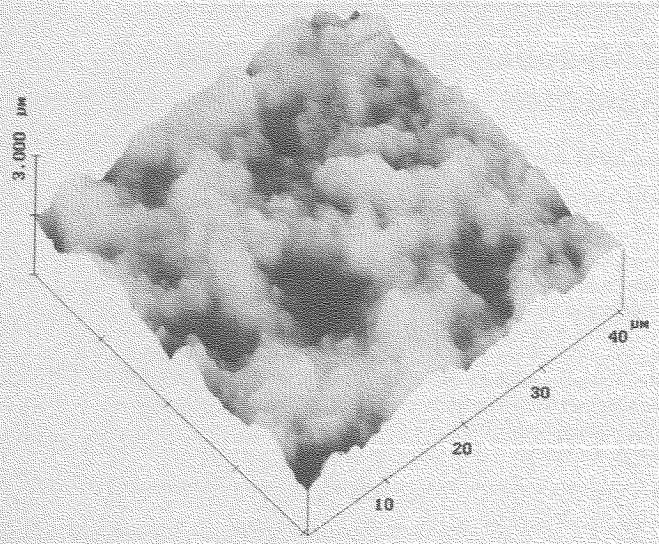

Figure 1. AFM image of a biofilm covered sample after 20 days.

AFM study.—For biofilm imaging, coupons were removed from the media, lightly rinsed in sterile distilled water, and then left to air dry. To reveal the extent of steel biocorrosion, the biofilm was removed by immersing the coupons in an ultrasonic bath for 5 min and then in passive Clarke solution[22] (36% HCl 1 L, Sb_2O_3 20 g, $SnCl_2$ 50 g) for 10−15 s to remove the corroded products. The exposed coupons steel surfaces were finally rinsed with sterile water, cleaned in 100% ethanol, and dried under nitrogen flow. Samples were examined by using a Nanoscope IIIA AFM (Digital Instruments, USA) in the tapping mode with the standard etched silicon probes. The AFM probe has a cantilever length of 125 µm and tip radii of curvature of 5-10 nm. The sides of the tip make an angle of 17° with the vertical while the front face and back face are 25 and 10° with the vertical line, respectively.

Results and Discussion

Biofilm.—Under anaerobic conditions, a biofilm is formed in the absence of dissolved oxygen within days in sea water sustaining SRB culture. This biofilm acts as a barrier to diffusion, resulting in the creation of gradients of pH, sulfate, and chloride. Figure 1 shows a 20 day old biofilm composed of marine SRB formed on the steel surface. The biofilm consists of clusters of microbial cells, EPS, and interstitial voids. A recent study,[23] using confocal scanning laser microscope (CSLM), estimated that bacterial cells only occupied 5 to 25% of the biofilm volume. The heterogeneity of biofilm gives significantly greater mean surface roughness (144.7 nm) compared to the smaller roughness (3.4 nm) of the original coupon. In addition to its structure, the composition of the biofilm also plays an important role in biocorrosion. In this study, SRB utilizes lactate as an energy source and oxidizes it first to pyruvate, then to acetate and CO_2.[24] This is coupled with the reduction of sulfate to sulfide. Metal sulfide is deposited and adhered to the metal surface and constitutes part of the biofilm. The precipitation of biogenic sulfide inhibits a protective film formation. The contribution of sulfide to biocorrosion has been reviewed by Lee *et al.*[25] The EPS secreted by two different isolates of marine SRB was characterized by Zinkevich *et al.*[13] Proteins, uronic acids, neutral hexoses, and amino sugars were the major EPS components observed, and composition of EPS matrix was affected by the carbon steel surface present.

Determination of depth and volume of pits.—Section and bearing analyses of Nanoscope IIIA allow for conveniently measuring of the depth and volume of a pit after removal of biofilm and deposits. Figure 2 illustrates a typical corrosion pit cross section and bearing

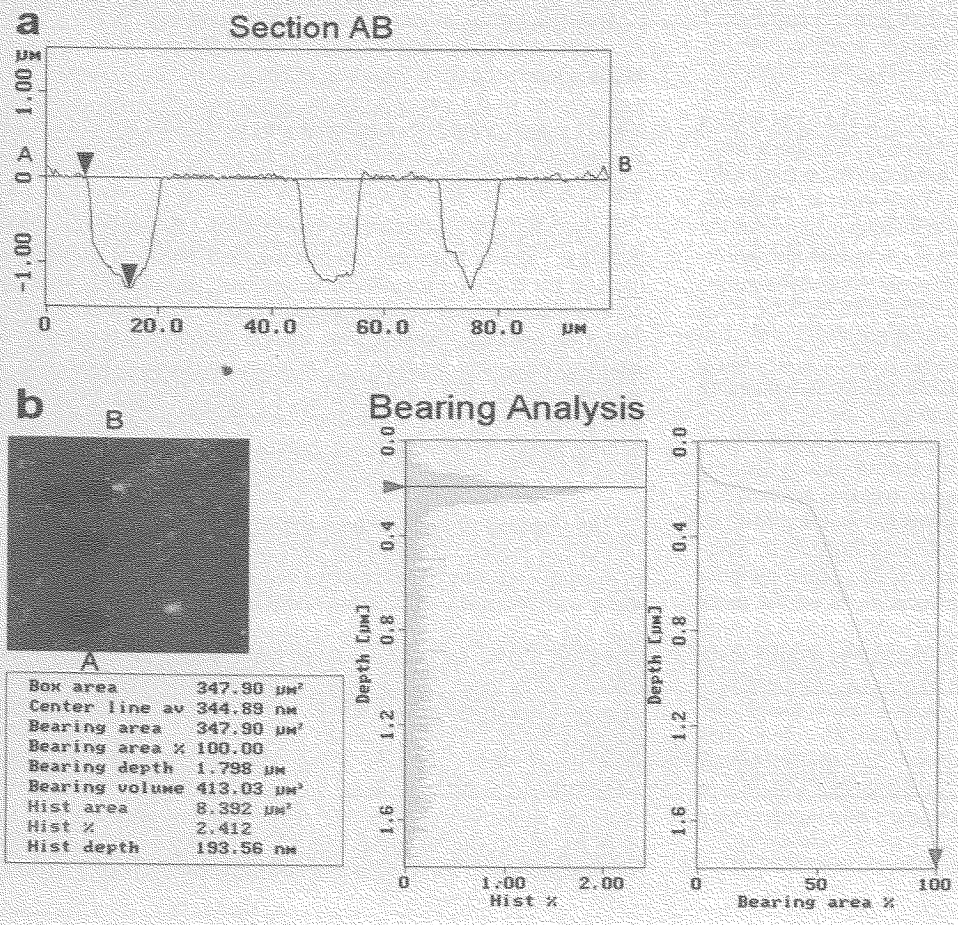

Figure 2. Section and bearing analysis of typical corrosion pits of mild steel after immersion in SRB culture for 50 days: (a) vertical distance of two cursors in the cross section AB is 1.33 µm; (b) volume determination of the pit by bearing analysis.

S0013-4651(99)01-006-X CCC: $7.00

analysis. The maximum vertical distance of the pit from the surface was taken as the depth of pit (section AB in Fig. 2a). The section analysis was performed three times at different orientations and the largest dimension measured was adopted as the representative depth for each pit. Before analysis, all the scanned images were flattened and plane fit.

The bearing is defined as the amount of the scanned area that lies above a given height (bearing depth). Figure 2b shows a typical bearing analysis. The bearing area is equal to the box area. The volume of pit can be calculated by

$$\text{Volume of pit } (\mu m^3) = (\text{bearing area}) \times (\text{bearing depth}) - (\text{bearing volume})$$

The stop band command is adopted to remove the influence of minute debris on the surface in the bearing calculation.

Pits and quantitative determination of biocorrosion.—After removal of the biofilm and deposits, numerous pits can be found on the coupon surface by AFM scans. Figure 3 shows the progression of pitting in coupons of different stages. No surface damage could be

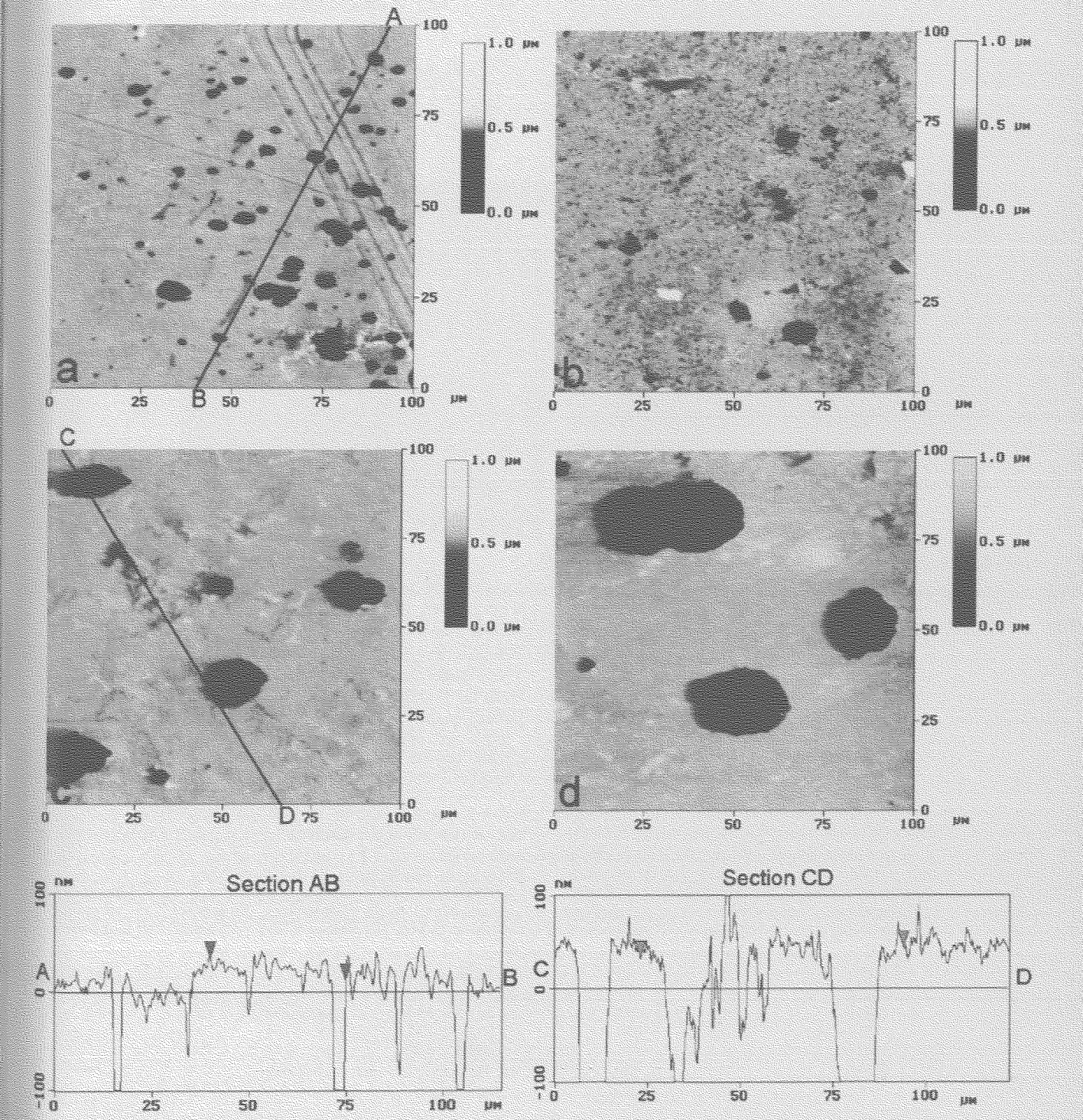

Figure 3. AFM images of coupons surface corroded for different periods. (a) 10, (b) 30, (c) 40, and (d) 60 days. (Section AB of 3a and CD of 3c are shown at the bottom.)

S0013-4651(99)01-006-X CCC: $7.00 © The Electrochemical Society, Inc.

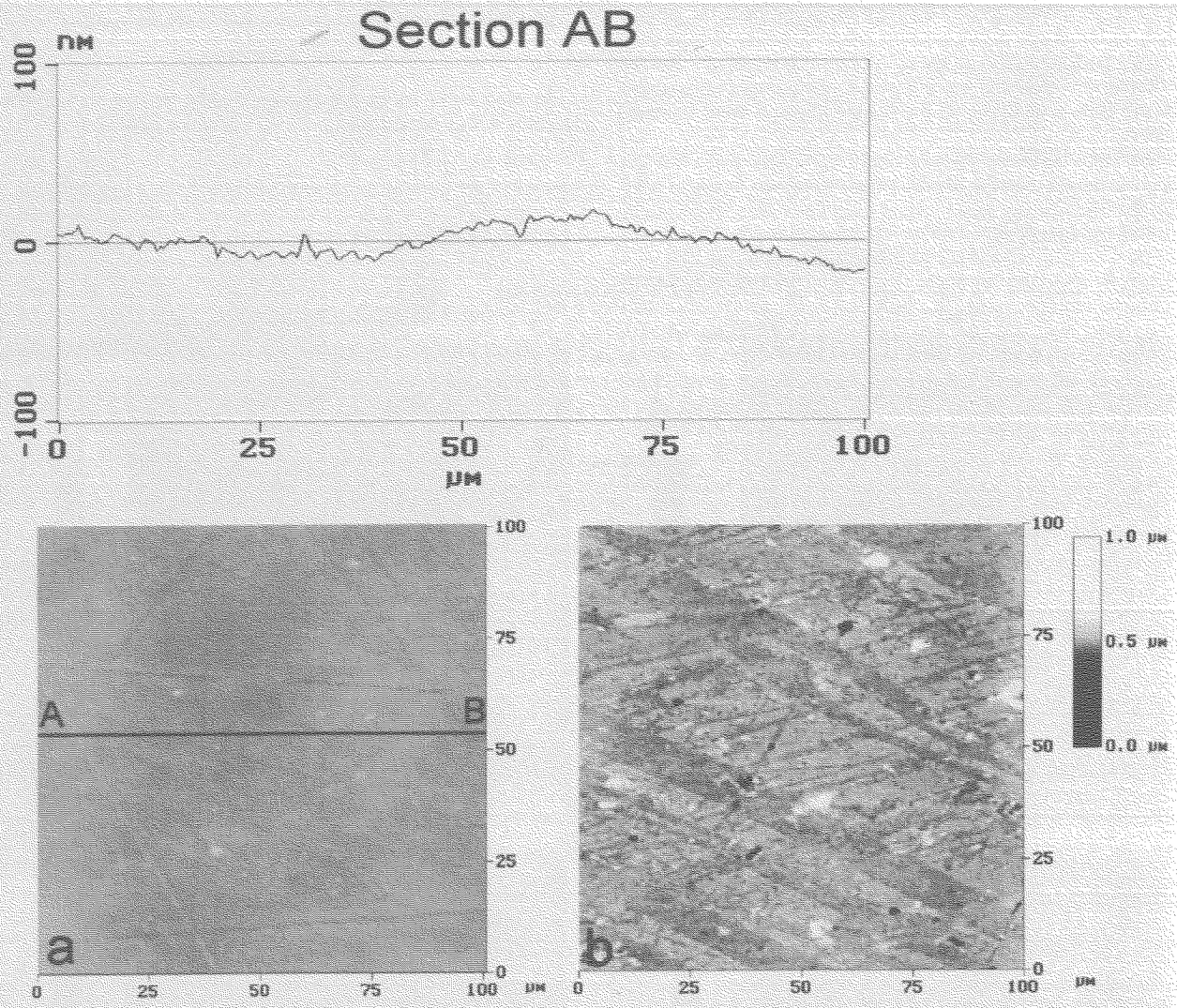

Figure 4. AFM images of a control coupon surface. (a) Initial coupon, the cross-sectional profile along the line AB is displayed; (b) after immersion for 60 days.

seen in corresponding control samples (no SRB) in the first 20 days. After 60 days, the pit generated on the surface of the control sample (Fig. 4) was much smaller than that with MIC. After 10 days the mean surface roughness of steel coupons stripped of biofilm is 27.8 nm compared to the initial roughness of 3.4 nm. As corrosion progressed, the width and depth of pits increased. The apparent higher density of pits in Fig. 3a compared to later images is due to the change of vertical scale, contrast, and focus offset in the image display. Theoretically, the number of pits per unit area (density of pits) can be analyzed from the AFM image. As corrosion progressed, much deeper and wider pits appeared. Some pits merged together while new pits formed. The initial surface became very rough and identification of small pits became obscure, especially near the mouth of a big pit. Section CD in Fig. 3 is much more rugged than

Table I. The measured results of pits through AFM in the different corrosion periods.

Time (day)	Total pit volume of scanned area (μm^3/100 × 100 μm)	Density (No./10 × 100 μm)	Volume (μm^3/pit) (Mean ± SD)[a]	Area (μm^2/pit) (Mean ± SD)	Depth (μm/pit) (Mean ± SD)	Ratio of V/(AD)[b]	Corresponding weight loss (mg/cm^2)[c]
10	117.4	27.3	4.28 ± 3.54	30.46 ± 11.81	0.37 ± 0.14	0.38	0.0092
20	160.6	25.8	15.2 ± 17.4	53.39 ± 38.57	0.44 ± 0.28	0.73	0.0125
30	203.0	27.6	43.9 ± 42.8	79.55 ± 52.81	0.84 ± 0.53	0.66	0.0158
40	595.3	21.5	275.7 ± 207.6	332.1 ± 170.1	1.39 ± 0.64	0.60	0.0464
50	993.2	24.2	359.3 ± 209.4	383.6 ± 156.4	1.96 ± 0.71	0.48	0.0755
60	1234.9	22.3	459.3 ± 271.5	413.2 ± 192.4	2.11 ± 0.76	0.53	0.0963
Mean	—	24.8	—	—	—	0.56	—

[a] SD: standard deviation.
[b] V = volume, A = area, D = depth.
[c] Weight loss is calculated from the total pit volume of scanned area (100 × 100 μm). The density of mild steel is taken as 7.8 g/cm^3.

S0013-4651(99)01-006-X CCC: $7.00 © The Electrochemical Society, Inc.

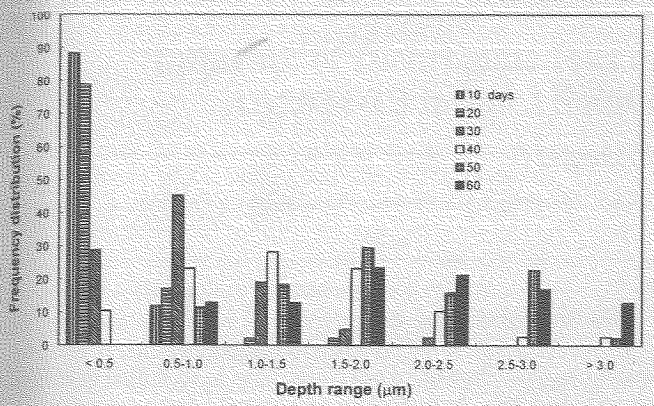

Figure 5. Variation of pit depth distribution with corrosion period.

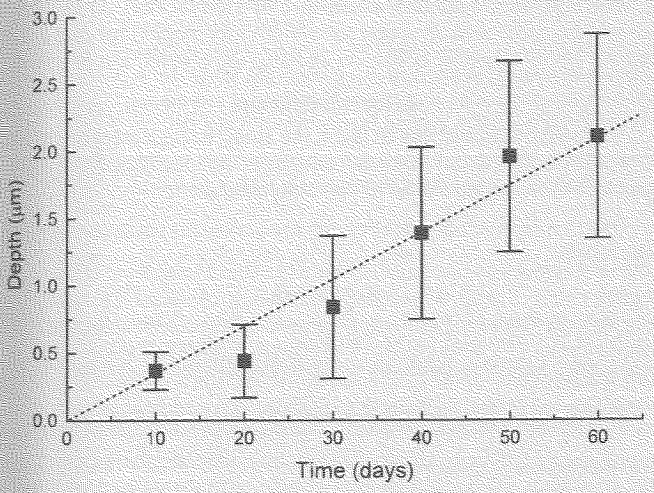

Figure 6. The relationship of depth and time. (The error bars show standard deviations of pit depths for the same surface.)

section AB and the identification of the smaller pits is more difficult. Nevertheless, an effort has been undertaken to count pits that are at least 1-2 μm wide and 0.1 μm deep in the scanned images and are tabulated in Table I. Actually, the density of pits changed little in the different periods. A more meaningful index of the extent of corrosion may be the total pit volume of the scanned area. This can be obtained by bearing analysis and are tabulated in Table I. The weight loss corresponding to this volume change can be calculated. Figure 5 shows the distribution of pit depth for images corroded after 10, 20, 30, 40, 50, and 60 days. The mean depth of pits increased with time, as shown in Fig. 6. From the distribution in Fig. 5, about 88.2% of pits are less than 0.5 μm deep, and no pit deeper than 1.0 μm is observed for 10 day coupons. For the 60 day coupon, more than half of the pits are over 2.0 μm in depth and 12.8% have depths larger than 3.0 μm. Figure 6 shows the depth of pits increased linearly with time. Based on these data, the average pit growth rate for mild steel due to MIC in anaerobic seawater containing SRB is 12.0 μm/year.

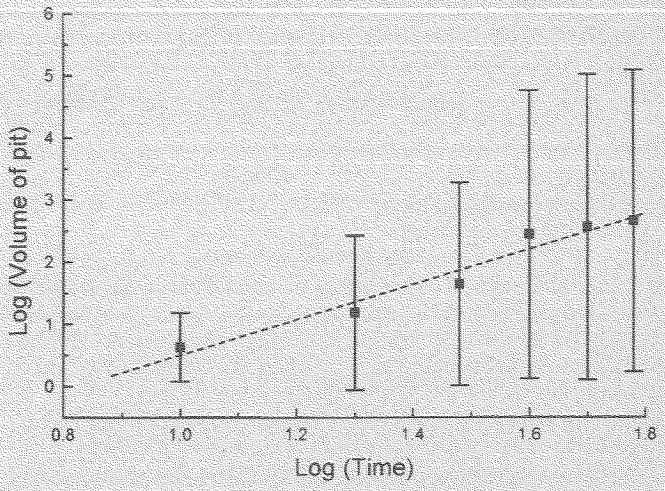

Figure 7. Power law fitting of pit volume *vs.* time assuring volume = a (time)^b. (The regressed parameters are $a = 0.0047$, $b = 2.83$. The error bars show standard deviations of pit volumes for the same surface.)

The corresponding average corrosion rate, based on volume loss in Table I, however, is 0.49 μm/year.

AFM has a higher resolution and accuracy in the vertical dimension compared to other microscopy techniques and is useful in probing the morphological change of individual pits. To understand the growth of individual pits, the depth, mouth area, and volume of the larger representative pits at various corrosion stages were studied with the bearing analyses. The results are tabulated in Table I. Through a full log regression in Fig. 7, the volume of the pit grows as 0.0047 (time)$^{2.83}$. The ratio of volume to the product of area and depth suggests the shape of corroded pits is neither a cone nor cylinder, but usually a combination of these two shapes as shown in Fig. 2a.

No pits can be observed in the control samples on days 10 and 20. The mean depth of pits in the control samples is about one order of magnitude smaller than corresponding MIC samples at the same time, as shown in Table II. The deterioration of mild steel is mainly caused by the biological attack in anaerobic seawater, but there is no quantitative link between SRB numbers or activity and the corrosion rate.[26] The microorganisms do not participate in the corrosion process directly but are able to actively change the environment surrounding the metal surface to facilitate the corrosion process. With the biofilm removed, the steel surface was found to be covered with a dark blue deposited film. The energy dispersive X-ray (EDX) analysis results indicated that this film is mainly constituted of iron sulfide. The physical and chemical properties of iron sulfide would affect the corrosion rate of mild steel. A thin, adherent, continuous sulfide film would be protective. However, there was no protective film formed beneath the biofilm. The scanning electron microscopy (SEM) in Fig. 8 showed sulfide film deposited nonuniformly near the pit on the steel surface. EDX analysis results showed the content of sulfur around the pit was 4.22% compared to 0.37% in region A inside of pit. A galvanic cell was established with steel behaving as the anode and the solution/iron sulfide interface as the cathode. The cathodic reaction is the reduction of the sulfate ion to the sulfide ion

Table II. The mean depth of pits for MIC and control samples (mean ± SD, μm).

Time (days)	10	20	30	50	60
MIC	0.37 ± 0.14	0.44 ± 0.27	0.84 ± 0.53	1.96 ± 0.71	2.11 ± 0.76
control	ND	ND	0.083 ± 0.027	0.19 ± 0.10	0.31 ± 0.12

SD: standard deviation.
ND: not detected.

Journal of The Electrochemical Society, **146** (12) 4455-4460 (1999)
S0013-4651(99)01-006-X CCC: $7.00

Table III. Weight loss of coupons in anaerobic seawater containing SRB.

	(coupon: 40 × 15 × 1.5 mm)				
Time (days)	15	30	45	60	75
Weight loss (mg/cm^2)	0.095	0.110	0.154	0.637	1.121
Corrosion rate (mg/dm^2/day)	0.635	0.366	0.342	1.062	1.495

in the presence of SRB. The electron is supplied from the FeS solid phase. The probable anodic reaction is dissolution of iron to free ions with the creation of pits. The smaller area of anode relative to cathode leads to higher current density, higher dissolution rate, and deepening of pits. The ferrous ions formed may deposit as FeS outside the pit in the presence of sulfide ions. The other possible anodic reaction is the direct formation of iron sulfide. This requires diffusion of sulfide ions through the solid phase and is unlikely to occur at a later stage of corrosion when the FeS film is thick. Furthermore, the absence of iron dissolution does not support the picture of pit formation. The effect of iron sulfide formed in MIC on the corrosion rate of mild steel has been discussed by Lee and Characklis.[26]

Weight loss measurement and comparison with AFM analyses.—Weight loss measurements give the overall corrosion rate. This common method was used to measure biocorrosion recently.[27] Table III shows the results of weight loss experiments during 15, 30, 45, 60, and 75 days. Compared to the AFM results of Table I, these data are about one order of magnitude higher. The corresponding corrosion rates in Table III, however, show some scattering at the early days of corrosion. The weight loss method may be less accurate at the early stage of corrosion when the absolute weight change is too small to be determined accurately. On the other hand, the bearing analyses of AFM images suffers the loss of a relatively flat reference plane at the later stages and may underestimate the real corrosion. The AFM should be the better method for quantifying early corrosion, while at the same time revealing local corrosion phenomena. The weight loss method should be better for extended corrosion quantification.

Site	A	B	C	D
Fe (atom %)	99.63	95.78	98.74	98.53
S (atom %)	0.37	4.22	1.26	1.47

Figure 8. SEM image of corrosion pit and EDX analysis of sulfide around the pit.

Conclusion

Atomic force microscopy is a powerful method for analyzing the corrosion of steels in the presence of microorganisms. A heterogeneous biofilm composed of cell clusters can be identified in samples exposed to SRB. The depth of pits increased linearly with time and the volume of pits increased at the 2.83 power of time. In anaerobic seawater sustaining SRB, the local depth increase of larger pits of mild steel is 12.0 μm per year which is one order of magnitude larger than corrosion without the influence of SRB biofilm. AFM measurement is more sensitive than the weight loss method for determining the initial stages of corrosion and also the distribution of pitting.

Acknowledgments

The authors would like to thank the Hong Kong Research Grants Council for the partial financial support of this study and the assistance of C. Y. Leung for AFM characterization.

The University of Hong Kong assisted in meeting the publication costs of this article.

References

1. H. C. Flemming, in *Microbially Influenced Corrosion of Materials*, 1st ed., E. Heitz, H. C. Flemming, and W. Sand, Editors, p. 5, Springer, Berlin (1996).
2. D. Beer, P. Stoodley, F. Roe, and Z. Lewandowski, *Biotechnol. Bioeng.*, **43,** 1131 (1994).
3. W. Lee and D. Beer, *Biofouling*, **8,** 273 (1995).
4. B. Little and P. Wagner, in *Biofouling and Biocorrosion in Industrial Water Systems*, G. G. Geesey, Z. Lewandowski, and H. C. Flemming, Editors, p.213, Lewis Publishers, Boca Raton, FL (1994).
5. R. D. Bryant, W. Jansen, J. Boivin, E. J. Laisheley, and J. W. Costerton, *Appl. Environ. Microbiol.*, **57,** 2804 (1991).
6. S. M. Gerchakov, B. J. Little, and P. Wagner, *Corrosion*, **42,** 689 (1986).
7. W. H. Dickinson, F. Caccavo, B. Olesen, and Z. Lewandowski, *Appl. Environ. Microb.*, **63,** 2502 (1997).
8. W. H. Dickinson and Z. Lewandowski, Paper 291 presented at Corrosion '96, National Association of Corrosion Engineering, Houston, TX (1996).
9. R. L. Islander, J. S. Devinny, F. Mansfeld, A. Postyn, and H. Shih, *J. Environ. Engin.*, **117,** 751 (1991).
10. B. Little, P. Wagner, K. Hart, R. Ray, D. Lavoie, K. Nealson, and C. Aguilar, Paper 215 presented at Corrosion '97, National Association of Corrosion Engineering, Houston, TX (1997).
11. G. Chen and C. R. Clayton, *J. Electrochem. Soc.*, **144,** 3140 (1997).
12. G. Chen and C. R. Clayton, *J. Electrochem. Soc.*, **145,** 1914 (1998).
13. V. Zinkevich, I. Bogdarina, H. Kang, M. A. W. Hill, R. Tapper, and I. B. Beech, *Int. Biodeterior. Biodegrad.*, **37,** 163 (1996).
14. I. B. Beech and C. W. S. Cheung, *Int. Biodeterior. Biodegrad.*, **35,** 59 (1995).
15. F. Mansfeld and B. Little, *Corros. Sci.*, **32,** 247 (1991).
16. S. C. Dexter, D. J. Duquette, O. W. Siebert, and H. A. Videla, *Corrosion*, **47,** 308 (1991).
17. G. Chen, R. J. Palmer, and D. C. White, *Biodegradation*, **8,** 189 (1997).
18. P. J. Bremer, G. G. Geesey, and B. Drake, *Curr. Microbiol.*, **24,** 223 (1992).
19. A. Steele, D. T. Goddard, and I. B. Beech, *Int. Biodeterior. Biodegrad.*, **34,** 35 (1994).
20. I. B. Beech, C. W. Sunny Cheung, D. B. Johnson, and J. R. Smith, *Biofouling*, **10,** 65 (1996).
21. H. A. Videla, *Manual of Biocorrosion*, p. 252, Lewis Publishers, Boca Raton, FL (1996).
22. *Laboratory Corrosion Tests and Standards*, G. S. Haynes and R. Baboian, Editors, ASTM Standard G1-81, p. 507, ASTM, Philadelphia, PA (1983).
23. D. E. Calwell, D. R. Korber, and J. R. Lawrence, *J. Microbiol. Methods*, **15,** 249 (1992).
24. R. Singleton, Jr., in *The Sulfate-Reducing Bacteria: Contemporary Perspectives*, J. M. Odom and R. Singleton, Jr., Editors, p. 5, Springer-Verlag, New York (1993).
25. W. Lee, Z. Lewandowski, P. H. Nielsen, and W. A. Hamilton, *Biofouling*, **8,** 165 (1995).
26. W. Lee and W. G. Characklis, *Corrosion*, **49,** 186 (1993).
27. C. G. Peng and J. K. Park, *Corrosion*, **50,** 669 (1994).